Multi-wavelength observing of a forming solar-like star

S. G. Gregory [a] E. Flaccomio [b] C. Argiroffi [b] J. Bouvier [c] J.-F. Donati [d] E. D. Feigelson [e] K. V. Getman [e] G. A. J. Hussain [f] M. Jardine [a] F. M. Walter [g]

[a]SUPA, School of Physics and Astronomy, Univ. of St Andrews, St Andrews, KY16 9SS, U.K.

[b]INAF - Osservatorio Astronomico di Palermo, Piazza del Parlamento 1, 90134 Palermo, Italy

[c]Lab. d'Astrophysique, Univ. J. Fourier, CNRS, UMR 5571, BP 53, 38041 Grenoble, France

[d]LATT - CNRS/Univ. de Toulouse, 14 Av. E. Belin, F-31400 Toulouse, France

[e]Dept. of Astronomy and Astrophysics, 525 Davey Lab., Pennsylvania State Univ., University Park, PA 16802, U.S.A.

[f]ESO, Karl-Schwarzschild-Str. 2, Garching bei Muñchen, D-85748, Germany

[g]Dept. of Physics and Astronomy, Stony Brook Univ., Stony Brook, NY 11794-3800, U.S.A.

V2129 Oph is a 1.35 $M_\odot$ classical T Tauri star, known to possess a strong and complex magnetic field. By extrapolating from an observationally derived magnetic surface map, obtained through Zeeman-Doppler imaging, models of V2129 Oph's corona have been constructed, and used to make predictions regarding the global X-ray emission measure, the amount of modulation of X-ray emission, and the density of accretion shocks. In late June 2009 we will under take an ambitious multi-wavelength, multi-observing site, and near contemporaneous campaign, combining spectroscopic optical, nIR, UV, X-ray, spectropolarimetric and photometric monitoring. This will allow the validity of the 3D field topologies derived via field extrapolation to be determined.

1. Introduction

Classical T Tauri stars (CTTS) represent a key transitional period in the life of a star, between the embedded protostellar phase of spherical accretion and the main sequence stage. They are low mass pre-main sequence stars which accrete material from dusty circumstellar disks. They possess strong magnetic fields, of order a few kG [1], which truncate the disk and force in-falling gas to flow along the field lines. Material rains down on to the stellar surface, where it shocks and produces hotspots that emit in the optical, UV, and X-ray wavebands.

CTTS can be in excess of 1000 times more active in X-rays than the Sun is presently. X-rays from the central star may influence the dynamics and chemistry of the circumstellar disk, which will in turn set the initial conditions for planet formation, e.g. [2,3]. Understanding the distribution of the emitting plasma is important to assess the magnitude of these effects. The detection of rotationally modulated X-ray emission suggests that the bulk of the emitting plasma is confined within compact magnetic loops [4], but emission may also arise from large scale loops extending to several stellar radii [5]. Excess soft X-ray emission is another characteristic of CTTS [6]. However, in only 5 systems is this soft excess observationally associated with the dense plasma in accretion shocks (see [7] for a review). As a further indication of the complexity of CTTS, X-ray emission may also arise from shocks in outflowing bipolar jets [8].

In order to model X-ray emission from CTTS we require information about the magnetic fields that confine the coronal plasma and drive X-ray flaring via reconnection events. In this article we describe how models of the coronae of CTTS can be constructed via field extrapolation from surface magnetograms derived through Zeeman-Doppler imaging. We describe how a large multi-wavelength, multi-observing site campaign on the CTTS V2129 Oph will be used to test the ability of such models to capture the true 3D structure of CTTS magnetospheres, and their ability to predict X-ray emission properties.

2. ZDI and field extrapolation

Using the technique of Zeeman-Doppler imaging (ZDI) it is possible to map the medium and large scale structure of stellar magnetic fields (see [9] for a review of the technique). For CTTS, such surface maps are constructed by monitoring the rotational modulation of the Zeeman signal in both photospheric absorption lines, and emission lines which form at the accretion shock. Fig. 1 shows an example magnetic surface map of the CTTS V2129 Oph. The magnetic field of this star was found to be dominantly octupolar, with a contribution from many higher order field components [10].

By assuming a potential field the 3D structure of CTTS magnetospheres can be determined via field extrapolation from observationally derived magnetic surface maps [11]. Fig. 1 shows such an extrapolation from the magnetic map of V2129 Oph [10,12]. A clear distinction can be made between the complex surface field regions, with contains the $\sim 10^7$ K plasma that constitutes the X-ray emitting corona, and the somewhat simpler larger scale field that interacts with the circumstellar disk. The larger scale field, however, is distorted close to the stellar surface by the strong and complex surface field regions [11].

3. Modeling the stellar X-ray emission

The bulk of the X-ray emission from CTTS is thought to arise from magnetic reconnection events (flares) in a scaled-up solar-like coronae [13]. Once the structure of the surface magnetic field has been determined via field extrapolation, models of the distribution of X-ray bright regions can be constructed [14]. If we assume that the coronal plasma along each field line loop is in hydrostatic equilibrium then the gas pressure is given by,

$$p(s) = p_0 \exp\left(\frac{\mu m_H}{k_B}\int_s \frac{\mathbf{g}\cdot\mathbf{B}}{BT} ds\right), \qquad (1)$$

where p_0 is the base pressure at the stellar surface (at the loop footpoints), s is the coordinate along the loop, and the field vector $\mathbf{B}$ is calculated at each point within the stellar magnetosphere by field extrapolation [12]. The coronal plasma can either be assumed to be isothermal, or the temperature along individual loops scaled according to the loop length and base pressure. At each point along the field line loops we calculate the plasma-β, the ratio of gas to magnetic pressure. If $\beta > 1$ at some point along a field line then the loop is assumed to be unable to contain the coronal plasma, and is distorted and blown open, and is therefore dark in X-rays. Thus there is an inhomogeneous distribution of X-ray bright regions across the stellar surface. The X-ray dark areas contain the footpoints of wind bearing open field lines, and those of the larger scale field lines which interact with the disk. The latter regions, however, may also contain accretion shocks that emit at softer X-rays energies (see below). Once the pressure (or equivalently the gas number density

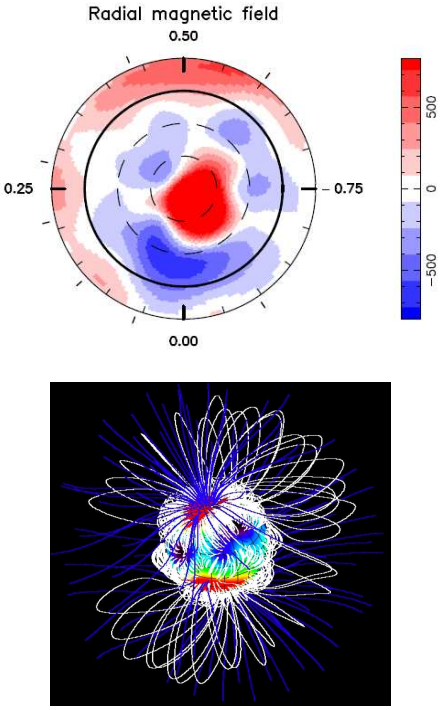

Figure 1. *Top panel*: A flattened polar projection of the surface magnetic topology of the accreting T Tauri star V2129 Oph, with the equator depicted as a bold circle [10]. *Bottom panel*: Red (blue) corresponds to positive (negative) field polarity with the fluxes labeled in Gauss. A field extrapolation showing the simple large scale field which interacts with the circumstellar disk, and the complex surface field which contains X-ray emitting plasma. Open field lines are blue, with closed field lines in white.

n_e) is known at each point within the corona the global X-ray emission measure (EM) can be obtained,

$$EM = \int\int\int n_e^2 dV = \frac{1}{4k_B^2}\int\int\int \frac{p^2}{T^2} dV. \quad (2)$$

From the extrapolated magnetic field of V2129 Oph, assuming an isothermal corona at 30 MK, we calculate an X-ray EM of $\log EM = 53.9\,\mathrm{cm}^{-3}$. Although this is large for a prototypical $0.5\,\mathrm{M}_\odot$ T Tauri star, it is reasonable for a more massive star like V2129 Oph (see [13]), and agrees within a factor of three with the X-ray luminosity calculated from *ROSAT* data [15].

In addition to coronal X-ray emission, the cool but dense plasma at accretion shocks emit softer X-rays, e.g. [6]. By assuming that accretion occurs at a steady rate along the larger scale field lines, and that mass and magnetic flux are conserved along each accreting flux tube, the number density of the accreting gas along the field lines connecting the disk to a particular hotspot can be determined from,

$$n(r) = \frac{1}{\mu m_H}\frac{B(r)}{B(R_*)}\frac{\dot{M}}{A_* v(r)}, \quad (3)$$

where $\dot{M}$ is the fraction of the total disk accretion rate in to the particular hotspot that covers an area of the stellar surface of A_* [16,12]. Fig. 2 show some example density profiles along a selection of accreting field lines assuming that accretion occurs from a range of radii within the disk of V2129 Oph. The shock densities derived from the model are large enough to expect some soft X-ray emission from the accretion hotspots.

The few CTTS observed with high resolution X-ray spectroscopy, however, have shown very different average plasma temperatures. In order to understand what we may expect to observe we have simulated *Chandra* HETG spectra by considering two "extreme" cases: TW Hya, which has a cool corona ($T = 2.9, 8.0, 15.5$ MK and $EM = 19.2, 1.2, 3.1 \times 10^{52}\,\mathrm{cm}^{-3}$), and the hotter BP Tau ($T = 2.3, 7.3, 25.2$ MK and $EM = 3.5, 5.3, 10.3 \times 10^{52}\,\mathrm{cm}^{-3}$) as determined by [17]. The models are scaled to match the observed V2129 Oph X-ray flux determined from *ROSAT* data. Enlargements of the simulated HETG spectra for the hot and cool plasma models in the Ne IX and O VII triplet regions, assuming two different plasma densities, and an exposure time of 200 ks, are shown in Fig. 3. The hot model

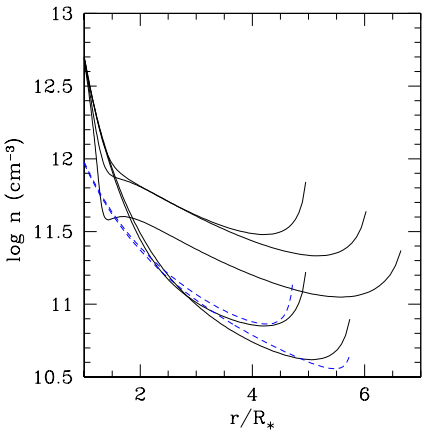

Figure 2. A steady state accretion flow model suggests that X-ray emission from accretion hotspots at the surface of V2129 Oph will be detectable [16,12]. The solid black lines represent the density structure of infalling gas flowing along the extrapolated field lines having left the inner disk from a range of radii. The dashed blue lines show the expected gas number density for accretion along dipolar field lines.

yields only ∼30 counts in the O VII triplet, but even in this case, from the expected number of counts in the lines and assuming Poissonian statistics, we would be able to distinguish with high confidence between typical coronal and accretion shock densities. For plasma densities larger than $\sim 10^{12}$ cm, for which the O VII indicator saturates, the Ne IX triplet can be used for the estimation. In the simulations we have ignored the X-ray background, negligible with respect to our expected source count rate.

4. Conclusions: testing the model with multi-wavelength observations

V2129 Oph has never been observed by *Chandra* or *XMM-Newton* . Our simulated accretion shock density based on a flow model using the magnetic field derived via field extrapolation indicates that X-rays from cool plasma at hotspots should be detectable, and distinguishable from the coronal contribution to the X-ray spectra. The *Chandra* data, to be obtained in late June 2009 (2×100 ks exposures separated by about half

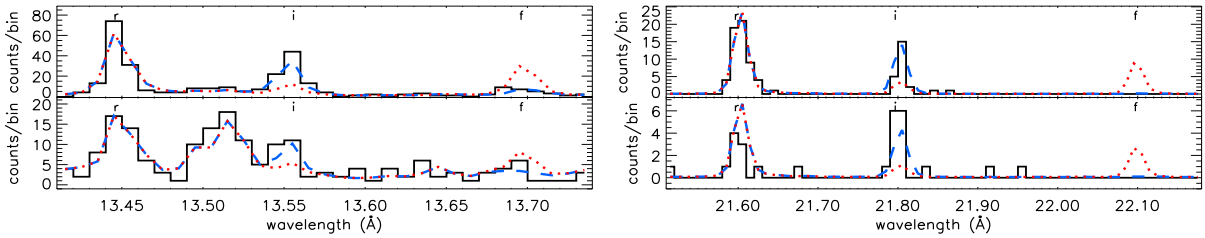

Figure 3. A simulation of the density sensitive Ne IX (*left panel*) and O VII (*right panel*) line triplets that form in the accretion shock for the cool/hot plasma model [*upper/lower panels*] assuming $\log n_e = 13\,\mathrm{cm}^{-3}$. The dashed (dotted) line indicates the noise-free spectra predicted for $\log n_e = 13(10)\,\mathrm{cm}^{-3}$.

a stellar rotation period), will therefore allow the predictions of the field extrapolation model to be tested. The surface magnetogram of V2129 Oph, however, was derived from spectropolarimetric data obtained with ESPaDOnS at CFHT in 2005 [10]. In order to account for possible variations in the magnetic field geometry of the star, we are scheduled to obtain new contemporaneous ESPaDOnS observations of V2129 Oph, with additional data from the twin instrument NARVAL at TBL in the French Pyrénées. A updated magnetic surface map will be derived using ZDI and new model predictions produced for direct comparison with the X-ray data.

The density of the plasma at the accretion shock determined from the model also depends on the assumed mass accretion rate, see equ. 3. Thus we will obtain additional optical and UV spectra from the HARPS instrument in the southern hemisphere, the KPNO 4m telescope and SMARTS (which will also provide photometric monitoring, allowing the distribution of hot/cool spots at the stellar surface to be inferred) in order to derive an accretion rate through veiling estimates. Furthermore, nIR spectra from CRIRES at VLT will allow Zeeman broadening measurements to better constrain the field strength at the surface of V2129 Oph, and will compliment the magnetic geometry determinations from the spectropolarimetric observations. The abundance of observational data will allow variability in the accretion related emission lines due to rotational modulation, and that due to time variable accretion, to be disentangled. The multi-wavelength, near contemporaneous data, in some cases covering several stellar rotation periods, will provide a crucial test of the ability of field extrapolation models to reproduce the true 3D nature of the magnetospheres of forming solar-like stars.

REFERENCES

1. Johns-Krull, C. M. 2007, ApJ, 664, 975.
2. Feigelson, E. D., Garmire, G. P., & Pravdo, S. H. 2002, ApJ, 572, 335.
3. Pascucci, I., Hollenbach, D., Najita, J. *et al.* 2007, ApJ, 663, 383.
4. Flaccomio, E., Micela, G., Sciortino, S. *et al.* 2005, ApJS, 160, 450.
5. Getman, K. V., Feigelson, E. D., Micela, G. *et al.* 2008, ApJ, 688, 437.
6. Telleschi, A., Güdel, M., Briggs, K. R. *et al.* 2007, A&A, 468, 443.
7. Güdel, M., & Nazé, Y. 2009, A&ARv, in press (astro-ph/0904.3078).
8. Güdel, M., Telleschi, A., Audard, M. *et al.* 2007, A&A, 468, 515.
9. Donati, J.-F., & Landstreet, J. D. 2009, ARA&A, in press (astro-ph/0904.1938).
10. Donati, J.-F., Jardine, M., Gregory, S. G. *et al.* 2007, MNRAS, 380, 1297.
11. Gregory, S. G., Matt, S. P., Donati, J.-F. *et al.* 2008, MNRAS, 389, 1839.
12. Jardine, M., Gregory S. G., & Donati, J.-F. 2008, MNRAS, 386, 688.
13. Preibisch, T., Kim, Y.-C., Favata, F. *et al.* 2005, ApJS, 160, 401.
14. Gregory, S. G., Jardine, M., Collier Cameron, A. *et al.* 2006, MNRAS, 373, 827.
15. Casanova, S., Montmerle, T., Feigelson, E. D. *et al.* 1995, ApJ, 439, 752.
16. Gregory, S. G., Wood, K., & Jardine, M. 2007, MNRAS, 379, L35.
17. Robrade, J., Schmitt, J. H. M. M. 2006, A&A, 449, 737.